Applied Energy 285 (2021) 116435

Contents lists available at ScienceDirect

Applied Energy

journal homepage: www.elsevier.com/locate/apenergy

Intelligent demand side management for optimal energy scheduling of grid connected microgrids

R. Seshu Kumar [a], L. Phani Raghav [a], D. Koteswara Raju [a], Arvind R. Singh [b,*]

[a] Department of Electrical Engineering, National Institute of Technology, Silchar, India
[b] School of Electrical Engineering, Shandong University, Jinan, China

HIGHLIGHTS

- Power sharing among energy resources in microgrid effectively coordinated by an EMS.
- Incorporation of DSM with EMS effects total operating cost and peak reduction.
- Proposed EMS framework solves optimal scheduling & minimizing operational cost.
- First stage addresses uncertainty problem considering real-time meteorological data.
- Second stage deals microgrid configuration, operational constraints and DSM load.
- QPSO is devised to obtain the optimal power dispatch configuration in microgrid.

ARTICLE INFO

Keywords:
Microgrid
Quantum Particle Swarm Optimization
Demand Side Management
Energy Management System
Stochastic optimization

ABSTRACT

The incorporation of renewables and communication technologies to the utility paves a way for self-sustained microgrids (MG). The volatile nature of these resources, uncertainties associated with the time-varying load, and market prices impose the significance of an efficient energy management system (EMS). So far, the MG optimal operation has been referred to optimize the operating costs only. However, the prospects of incorporating demand-side management (DSM) with the EMS problem and its effect on total operating cost and peak reduction is needed to be evaluated. To fill this gap, the impact of utility induced flexible load shaping strategy on non-dispatchable energy sources is investigated in this paper. A three-stage stochastic EMS framework is proposed for solving optimal day-ahead scheduling and minimizing the operational cost of grid-connected MG. In the first stage, four possible scenarios for solar and wind power generation profiles are created to address the uncertainty problem by considering real-time meteorological data. The second stage deals with the MG system configuration, operational constraints, and assigning DSM load participation data to be incorporated with the objective function. In this regard, the Quantum Particle Swarm Optimization is devised at stage three to obtain the optimal power dispatch configuration for DG units, maximizing the power export to the utility and compare the results with and without incorporating DSM participation for all scenarios. The obtained simulation results show the competence of the proposed stochastic framework about cost reduction by 43.81% with the implementation of the load participation level of 20% DSM.

1. Introduction

The commercial deployment of local distributed generation (DG) sources at the distribution network are growing at a rapid pace. The presence of DG in proximity to the loads can enhance the power quality, reliability, and economics of energy supply. Photovoltaic, wind turbine, fuel cell, microturbine, and battery energy storage systems are some examples of distributed energy resources that are interconnected with a cluster of controllable loads to form a microgrid. There will be a significant change in the operation and control strategies of microgrids compared to the conventional power system. The reasons are depending on the level of penetration of DG units and their characteristics, power quality constraints, and several market pricing strategies [1].

To realize the potential benefits of MG, a sophisticated energy management system is needed to effectively coordinate power output

* Corresponding author.
E-mail address: arvindsinghwce@gmail.com (A.R. Singh).

https://doi.org/10.1016/j.apenergy.2021.116435
Received 5 December 2020; Received in revised form 29 December 2020; Accepted 3 January 2021
Available online 12 January 2021

Nomenclature

χ	Vector of optimization variables
NG	Number of DG units
NS	Number of Energy Storage device
P^t_{DGi}	Active power output of i^{th} DG at hour t
B^t_{DGi}	Bid price of i^{th} DG at hour t
S_{DGi}	Start/Shutdown costs for i^{th} DG unit
P^t_{ESj}	Active power output of j^{th} storage at hour t
B^t_{ESj}	Bid price of the j^{th} storage at hour t
S_{ESj}	Start/Shutdown costs for j^{th} storage device
p^t_{ut}	Active power exchange between utility and MG at time t
B^t_{grid}	Bid of utility at hour t
P^t_{load}	Active power demand of load at hour t
$P^t_{DGi,min}$	Minimum power limit of i^{th} DG at hour t
$P^t_{DGi,max}$	Maximum power limit of i^{th} DG at hour t
$P^t_{ESj,min}$	Lower limit of j^{th} storage power at hour t
$P^t_{ESj,max}$	Upper limit of j^{th} storage power at hour t
$P^t_{g,min}$	Lower limit of the utility power at hour t
$P^t_{g,max}$	Upper limit of the utility power at hour t
P_{pv}	Active power output from the photovoltaic system
P_{WT}	Active power output from wind turbine
B_{ES}	Active power output from energy storage
$\mathcal{F}(t)$	Forecasted Load
$\mathbb{C}(t)$	Connected Load
Ã°(t)	Disconnected Load
$P^f_{pv,t}$	Forecasted solar power at hour t
$P^f_{wt,t}$	Forecasted wind power at hour t
$\Delta P_{pv,t,s}$	Solar forecast error at time t for scenarios
$\Delta P_{wt,t,s}$	Wind forecast error at time t for scenarios
N_s	Number of scenarios
N_T	Number of time intervals
$x_{i,j}$	Present position of i^{th} particle in j^{th} iteration
$p_{i,j}$	Pbest of i^{th} particle in j^{th} iteration
G_j	Gbest in j^{th} iteration
ξ	Contraction-Expansion coefficient
$mbest_{i,j}(t)$	Mean of *pbest* position
φ	Local focus point

List of Abbreviations

PV	Photovoltaic
WT	Wind Turbine
MT	Microturbine
FC	Fuel Cell
BESS	Battery Energy Storage System
MG	Microgrid
QPSO	Quantum Particle Swarm Optimization
DSM	Demand Side Management
EMS	Energy Management System

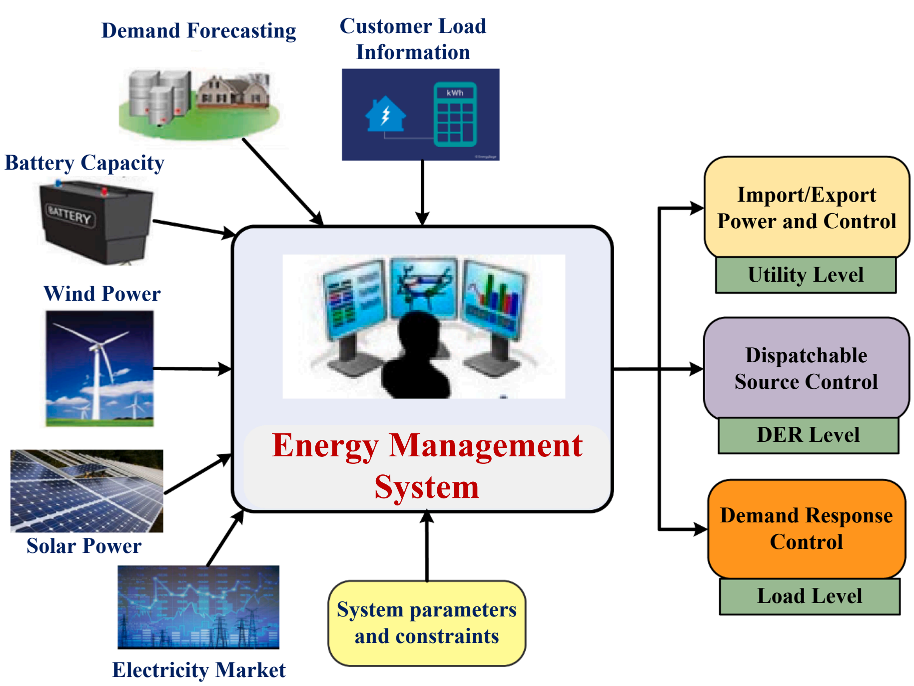

Fig. 1. Input information flow and functions of microgrid EMS.

among the interconnected DG units and to serve the critical and controllable loads cost-effectively [2]. The energy management in grid-connected and autonomous modes of MG differs as per the operational requirements. In the grid-connected mode, the prime objective of EMS is to maximize the revenues as per the DG bidding costs and market price, whereas in the autonomous mode of operation, the priority is given to provide a reliable supply to the critical loads by maximizing customer satisfaction [3]. The typical input information flow regarding utility market prices, forecast data of intermittent sources, system operational constraints, load data, and the functions of EMS is presented in Fig. 1.

Recently, numerous studies have addressed the optimal energy management problem under both deterministic and non-deterministic approaches. The deterministic models will not yield desired results for practical EMS problem which consists of weather-induced uncertainties while dispatching DG sources like Solar PV and wind. Hence, several non-deterministic approaches like stochastic programming, robust optimization, probabilistic models have been reported in the literature to solve the energy management and day-ahead optimal scheduling of non-dispatchable sources in the MG.

One way to address the uncertainties in the stochastic models is by generating scenarios to improve accuracy. Stochastic load flow based framework is employed in [4] to model the uncertain parameters of renewable sources in AC-DC hybrid MG. Also, to solve the EMS problem, energy losses and network voltage levels are evaluated in this work by employing the crow search algorithm. A robustness factor 'p-robust' is incorporated with a stochastic model in [5] to improve the accuracy of generated scenarios. The authors combined incentive-based and price-based DR programs to optimize the microgrid EM. In [6], a Markov decision framework is proposed by taking stochastic generation and load models into consideration. Naïve energy management policies are formulated to identify 'feasible decision space' by employing a stochastic dynamic programming approach. As discussed previously, researchers have shown interest to incorporate several new meta-heuristic algorithms with a stochastic framework to improve the effectiveness of EMS solutions. For example, new algorithms like Salp Swarm [7], modified Bat [8] are employed in recently published works and the results state that stochastic approaches yield desired optimized costs compared to deterministic models.

Unlike stochastic models, robust optimization considers an uncertainty dataset to quantify the variable nature of parameters without generating and reducing a large number of scenarios. Giraldo et al. [9] proposed a robust EMS framework using a convex mixed-integer second-order cone programming model. A new robustness parameter is introduced to obtain global robustness while creating the deterministic equivalent of random parameters instead of operating over multiple scenarios. A piece-wise decision rule-based robust optimization approach is proposed in [10] considering multiple factors related to uncertainty. Novel features such as polyhedral uncertainty space, aggregation of uncertainty factors, and partial-past decision rules are introduced to quantify the uncertainty set effectively. Although the proposed adjustable robust optimization yields better results compared to the deterministic approach, it has a certain limitation that the affine decision rules lead to over-conservative results. Most of the research works consider BESS as an independent scheduling energy resource by neglecting its application as a back-up unit. In [11], a real-time EMS model is presented to incorporate battery swapping action while scheduling EV batteries in a community microgrid. A novel Lyapunov optimization framework is proposed by the authors to address the stochastic variables in real-time effectively without relying on scenario generation and reduction process.

Numerous MGs are interconnected using different topologies to maintain the reliable generation and load balance in grid-connected as well as islanded modes. Owing to several security benefits and distinct features of networked MGs, several studies were conducted to address their operational flexibility and economic aspects. For instance, In [12], the probabilistic optimal scheduling problem of networked microgrids is solved using particle swarm optimization. Two DR programs namely time-of-use and real-time pricing were considered for economic analysis. The uncertain parameters in the system are tackled by creating scenarios using the Monte Carlo simulation approach. The authors in [13] proposed a two-stage hierarchical EMS strategy for networked microgrids by taking the uncertainties related to solar, wind, and market price into consideration. The risk-averse day-ahead hourly scheduling is evaluated during the first stage and in the second stage, a rolling horizon optimization strategy is applied for real-time dispatch of the networked microgrid. Nevertheless, the lower level hierarchical optimization framework is developed without considering forecasting uncertainties. In a similar work [14], the battery degradation cost model is incorporated with the optimal scheduling problem of networked MG. The effect of charging and discharging cycles on overall operating cost is analyzed and the designed framework is solved using the Rainflow algorithm.

In [15], Venayagamoorty et al. proposed an intelligent dynamic EMS controller to serve critical and non-critical loads in the presence of non-dispatchable DG units. The adaptive dynamic programming and reinforcement learning framework is designed to generate dispatch control signals and evaluated under different BESS state of charge conditions. The effectiveness of MG dispatch strategies is better off with enhancing generation and load forecasting accuracy. In this context, the authors in [16] adopted the adaptive neuro-fuzzy interface system to generate the PV and wind forecasting agents in a multi-agent EMS framework. The authors in [17] formulated the multi-objective MG EMS problem as mixed-integer linear programming in the GAMS environment. The annual net present costs and power losses were evaluated with demand response in this work. A fuzzy interface system is employed to tackle the complexities involved with the charging and discharging cycles of BESS in the optimization problem. None of the afore-mentioned works have considered demand response (DR) programming as a part of EMS objective while optimizing the operating costs. Hence, there is still an opportunity for improving the robustness of the solution by incorporating DSM programs in the system.

The effect of DR programming on MG operational costs alongside the component size optimization is investigated in [18]. The implementation of DR significantly reduced the energy storage within the scheduled period as well as the loss of generated energy. However, this results in a shortage of operational reserves. Ju et al. [19] presented a two-layer EMS framework by considering hybrid BESS degradation costs. The long term capital costs of battery and supercapacitor are converted into real-time short term costs to minimize MG operational cost under time-of-use (TOU) and dynamic pricing schemes. Mohammadjafari et al. incorporated an incentive-based DR program into the EMS cost function in [20]. Based on the proposed hourly power curtailment of individual customers, marginal benefits are provided in ranking order. In [21], the optimal scheduling of MG is coupled with distribution feeder reconfiguration to enhance operational performance. DR programs like TOU, load shifting, and demand bidding are added to the cost function in a convex optimization framework. The reliability and supply-balance instability problems posed by scheduling highly uncertain DG units need to be addressed with prompt DR actions, especially during peak hours.

The authors in [22] have considered the load priority list (LPL) to assign ranking for the critical loads while applying a load shedding scheme to optimize the energy transactions. The neuro-fuzzy based DSM model is designed to decide the type and amount of the load to be curtailed without compromising the relative importance of essential loads. Sliding time window based load shifting DSM algorithm is proposed in [23] for optimal dispatch of biomass energy based CHP. The impact of seasonal variation of solar irradiance and heating load on DSM is also noticed and the results state that the system performance increases with employing greater flexibility of dispatchable loads. One of the challenges faced by the MG operator is to procure the energy from the upstream distribution network with variable day-ahead market prices by providing an optimal bidding curve. With this regard, an information gap decision theory based bidding strategy is proposed in [24] considering market induced uncertainties. This model provides both risk-averse and risk-taking decision-making functions in the presence of DR programs.

In most of the recently published works [33,34], the focus of the microgrid EMS problem is confined to either a deterministic or probabilistic approach of solving the MG optimal scheduling to minimize the operation costs. The incorporation of DSM strategies with EMS is studied in limited works [35]. The utility induced DSM strategies can be implemented in the interest of investigating the impact of flexible load shaping on MG operating costs. Considering the DSM programs in the MG EMS problem can influence the energy consumption pattern and provides effective control of non-critical loads. This paper considers various DSM participation levels of residential loads to enhance the MG operating costs and power trading costs with the utility. Due to the volatile nature of renewable energy sources (RES), the scenario-based strategy is applied to address the uncertainty problem. The following contributions are made by the authors in this work to solve the day-ahead scheduling and energy management problem of the grid-connected microgrid.

- The three-stage scenario-based stochastic framework is proposed for the grid-connected microgrid to solve the optimal scheduling problem.
- DG resources such as PV, WT, FC, MT, BESS are integrated into the microgrid.
- Four different scenarios for RES are created with practical data based on the stochastic analysis.
- Utility induced DSM program is incorporated in the problem to further reduce the operating costs.
- The application of quantum-based computational intelligence to solve the optimal energy management of MG has not been reported in the literature. A detailed comparison of optimized results is shown for the cases with and without the participation of DSM by solving the EMS problem with the QPSO algorithm.

The organization of this paper is briefed as follows. Section 2 describes the problem statement along with MG operational constraints. The modeling of various DG units and their bid cost evaluation in the MG system is discussed in Section 3. Further, the uncertainty of PV and WT is addressed by creating scenarios based on stochastic formulation. Section 4 deals with the proposed three-stage stochastic EMS framework and solution methodology based on the QPSO algorithm. The simulation results obtained for solving MG EMS and a brief analysis on algorithm convergence characteristics and other research outcomes are discussed in Section 5. And finally, the relevant conclusion for this work is provided in Section 6.

2. Problem formulation

The day-ahead microgrid optimal scheduling problem would commence with the detailed representation of cost objective function followed by operational constraints of DG units that are interconnected to the utility. The main objective considered in this paper is to determine the optimal generation set points of DG units for minimizing the total cost subjected to demand response. The total costs include the fuel consumption of DG sources, unit startup costs, the market price related to a power exchange between the MG and grid. The mathematical model of this problem is represented as follows [25].

2.1. Objective function

$$\begin{aligned}\text{Min }\ F(\chi) &= \sum_{t=1}^{T} TC^t \\ &= \sum_{t=1}^{T}\left\{\sum_{i=1}^{NG}\left[u_i^t P_{DGi}^t B_{DGi}^t + S_{DGi}\left|u_i^t - u_i^{t-1}\right|\right] + \sum_{j=1}^{NS}\left[u_j^t P_{ESj}^t B_{ESj}^t \right.\right. \\ &\quad \left.\left. + S_{ESj}\left|u_j^t - u_j^{t-1}\right|\right] + p_{ut}^t B_{grid}^t\right\}\end{aligned} \tag{1}$$

$$\chi = \left[P_{DG1}^t, P_{DG2}^t, \cdots, P_{NG}^t, P_{ES1}^t, P_{ES2}^t, \cdots, P_{NS}^t, p_{ut}^t, u_1^t, u_2^t, \cdots u_{NG+NS}^t\right] \tag{2}$$

where the vector χ refers to key decision variables including active power of i^{th} DG unit and j^{th} storage unit with their related ON/OFF states. The bids of DG and storage units are denoted as B_{DGi}^t and B_{ESj}^t at hour t, p_{ut}^t is the active power exchange from/to utility at hour t, and the bid cost of utility at hour t is denoted as B_{grid}^t.

2.2. Operational constraints

2.2.1. Power balance

One of the fundamental constraints of the EMS problem is the active power balance constraint to ensure total active power generated by the DG units, BESS and utility must satisfy the total load demand.

$$\sum\nolimits_{i=1}^{t} P_{DGi}^t + \sum\nolimits_{j=1}^{t} P_{ESj}^t + P_{ut}^t = \sum\nolimits_{l=1}^{t} P_{load}^t \tag{3}$$

2.2.2. Active power generation capacity

The minimum and maximum range of active power generation for all DG sources in MG and utility are specified as follows:

$$\begin{cases} P_{DGi,min}^t \le P_{DGi}^t \le P_{DGi,max}^t \\ P_{ESj,min}^t \le P_{ESj}^t \le P_{ESj,max}^t \\ P_{g,min}^t \le P_{ut}^t \le P_{g,max}^t \end{cases} \tag{4}$$

Eq. (4) is verified to ensure none of the DG units, storage devices and utility has violated their limits and in case of violation, the power units are fixed upon their upper/lower limits. To enforce the power balance constraint, P_{ut}^t is considered as a dependent variable and the new variable $P_{g,lim}^t$ is added.

$$P_{g,lim}^t = \begin{cases} P_{g,max}^t \, if \, P_{ut}^t > P_{g,max}^t \\ P_{g,min}^t \, if \, P_{ut}^t > P_{g,min}^t \\ P_{ut}^t \, if \, P_{g,min}^t \le P_{ut}^t \le P_{g,max}^t \end{cases} \tag{5}$$

The quadratic penalty factor term λ_{pen} is included with the objective function to handle the inequality constraints to decline the unfeasible solutions [26].

$$\text{Min }\ F(\chi) = \sum_{t=1}^{T} TC^t + \lambda_{pen}\left(P_{ut}^t - P_{g,lim}^t\right)^2 \tag{6}$$

2.2.3. Energy storage limits

Eqs. (7) and (8) represents the state of charge and the restriction imposed on the rate of charging/discharging of the battery storage unit.

$$W_{ES,t} = W_{ES,t-1} + \eta_{ch} P_{ch} \Delta t - \frac{1}{\eta_{dch}} P_{dch} \Delta t \tag{7}$$

$$\begin{cases} W_{ES,min} \le W_{ES,t} \le W_{ES,max} \\ P_{ch,t} \le P_{ch,max}; P_{dch,t} \le P_{dch,max} \end{cases} \tag{8}$$

where $W_{ES,t}$ and $W_{ES,t-1}$ are the amount of energy stored at time interval t and $t-1$, respectively. $P_{ch}(P_{dch})$ and $\eta_{ch}(\eta_{dch})$ are permitted rate of charge (discharge) and efficiency of the storage device during the charge (discharge) at a definite time Δt. $W_{ES,min}(W_{ES,max})$ and $P_{ch,max}(P_{dch,max})$ are the minimum (maximum) limits of energy storage and upper limit of charge (discharge) rate of energy storage.

2.3. Demand side management approach

The DSM strategies play a significant role in improving the economics of distribution network operators by modifying consumers' load profile. DSM programs are classified as customer induced and utility induced schemes. The flexible load shaping is the most preferable strategy among utility induced DSM to fully exploit the time independence of controllable loads [29,30]. The central DSM controller receives the load forecast data and evaluates the necessary actions for obtaining the desired load profile. During the hourly dispatch, the customer participates in the DSM program and receives scheduling signals through a two-way communication [31]. Thus, the flexible load shaping DSM strategy is incorporated as an integral objective of the day-ahead energy management problem to reduce system peak and overall operating cost. The purpose of implementing the DSM technique is to modify the

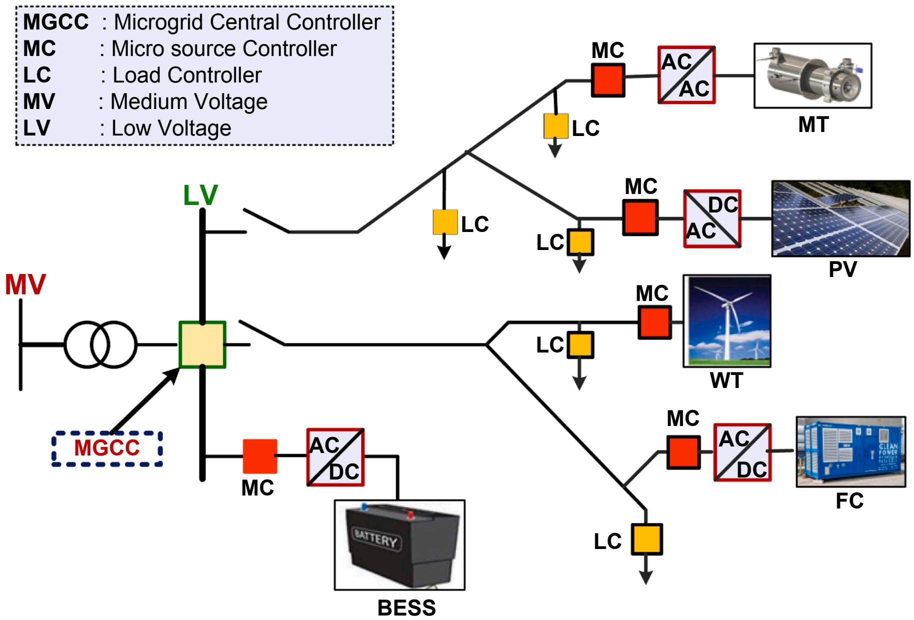

Fig. 2. Typical LV Microgrid System.

targeted load consumption profile close to the desired load profile as formulated below [29].

$$\min\ F = \sum_{t=1}^{T} (\varepsilon(t) - \delta(t))^2 \tag{9}$$

$$\varepsilon(t) = \mathcal{F}(t) + \mathbb{C}(t) - \tilde{A}^{\circ}(t) \tag{10}$$

where $\varepsilon(t)$ is the targeted load given as an input to the DSM controller and $\delta(t)$ is the desired load profile at time interval t. $\mathcal{F}(t)$, $\mathbb{C}(t)$, and $\tilde{A}^{\circ}(t)$ is the forecasted load, connected load, and disconnected loads at time interval t respectively.

$$\mathbb{C}(t) = \sum_{i=1}^{t-1} \sum_{l=1}^{N} \aleph_{iit} \cdot P_{1l} + \sum_{j=1}^{k-1} \sum_{i=1}^{t-1} \sum_{l=1}^{N} \aleph_{li(t-1)} \cdot P_{(1+j)l} \tag{11}$$

The connected load is based on increment in load from time slot i to t by shifting $\aleph$ number of l type controllable loads. P_{1l} and $P_{(1+j)l}$ is the active power consumed by l type devices at 1 and $(1+j)$ time steps, respectively. k is defined as a total time duration of load consumption for l type device.

$$\tilde{A}^{\circ}(t) = \sum_{q=t+1}^{t+m} \sum_{l=1}^{N} \aleph_{ltq} \cdot P_{1l} + \sum_{j=1}^{k-1} \sum_{q=t+1}^{t+m} \sum_{l=1}^{N} \aleph_{l(t-1)q} \cdot P_{(1+j)l} \tag{12}$$

The disconnected load is based on decrement in $\aleph$loads that are delayed from time slot t to q which are originally supposed to be consumed at time step t. Here m denotes the maximum allowable delay. The other constraints included for successful implementation of the DSM program are given as follows.

$$\sum_{t=1}^{T} \aleph_{lit} \le \aleph(i) \tag{13}$$

$$P_{(1+j)l} = 0, \quad \forall (1+j)l > T_D \tag{14}$$

$$\aleph_{lit} = 0, \quad \forall i > t; (t-i) > m \tag{15}$$

Eq. (13) represents that the number of l type devices must not exceed the number of controllable devices. T_D is the total time duration for load consumption of l type devices and the delayed characteristic of the DSM approach is shown in equation (15).

3. Modelling of DG units in microgrid

A typical low voltage grid-connected microgrid considered for evaluation of the proposed framework is shown in Fig. 2. The power exchange between MG and utility will be monitored and controlled by a microgrid central controller (MGCC). The key function of MGCC is to assign power references to the local controllers to satisfy power balance constraints for the scheduled period T. The micro-source controller (MC) and load controller (LC) must fulfill the power requirement by absorbing (supplying) the excess (deficit) energy supported by storage devices against the forecasting uncertainties. The system includes various DG units such as PV, WT, FC, MT, and energy storage devices.

3.1. Solar PV model

The PV system power output is subjected to vary with metrological parameters like solar irradiance I_s and ambient temperature T_a in the location and module characteristics. The estimation of power output P_{pv} from the PV module is given as follows [26].

$$P_{pv} = P_{STC} \frac{I_s}{1000} (1 + \alpha(T_c - 25)) \tag{16}$$

where P_{STC} is the maximum power (W) extracted from the module, I_s is the solar irradiance (W/m^2), T_c is the module temperature (°C), and α is the temperature coefficient (^{0}C^{-1}) for power from the PV module.

The PV module temperature for any given location can be estimated as a function of I_s and T_a based on the nominal value of the cell temperature T_N (^{0}C).

$$T_c = T_a + \frac{I_s}{800} \cdot (T_N - 20) \tag{17}$$

The hourly solar irradiance usually follows a Beta PDF $f_{pv}(\zeta)$ as presented in (18). The shaping parameters of this function α, β are evaluated in (19) and (20) using mean (μ) and standard deviation (σ) of the random variable ζ, which represents the solar irradiance.

$$f_{pv}(\zeta) = \begin{cases} \dfrac{\Gamma(\alpha+\beta)}{\Gamma(\alpha)\Gamma(\beta)} & \zeta^{\alpha-1}(1-\zeta)^{\beta-1} \\ 0 & otherwise \end{cases} \tag{18}$$

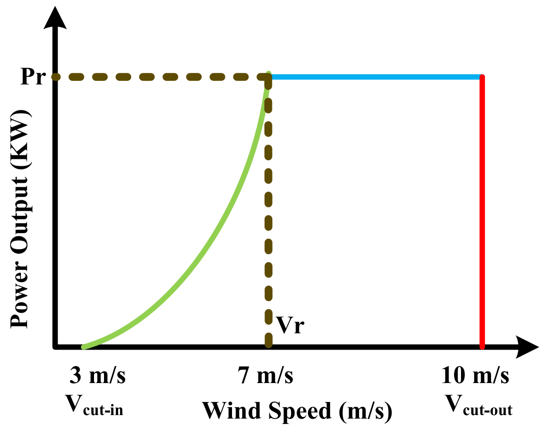

Fig. 3. Wind power characteristics.

$$\beta = (1-\mu)\times\left(\frac{\mu(1+\mu)}{\sigma^2}-1\right) \tag{19}$$

$$\alpha = \frac{\mu\times\beta}{1-\mu} \tag{20}$$

The probability of a discrete state with irradiance limits ζ_1, ζ_2 for solar uncertainty modeling is estimated in (21) during any specific time.

$$\rho(\zeta) = \int_{\zeta_1}^{\zeta_2} f_{pv}(\zeta)\cdot d\zeta \tag{21}$$

3.2. Wind uncertainty model

The power generated from the WT primarily depends on the intermittent nature of wind. The Weibull distribution is widely adopted to signify the timely variations of wind speed [26]. The Weibull probability distribution function is given as:

$$f_v(v) = \begin{cases} \frac{\beta}{\gamma}\times\left(\frac{v}{\gamma}\right)^{\beta-1}\times e^{-\left(\frac{v}{\gamma}\right)^{\beta}} & v\geq 0 \\ 0 & otherwise \end{cases} \tag{22}$$

The real power generated from WT based on the simulated wind velocity is represented as follows.

$$P_{WT} = \begin{cases} 0 \quad 0\leq v\leq v_{ci} \quad or \quad v\geq v_{co} \\ \frac{v^2-v_{ci}^2}{v_r^2-v_{ci}^2}\times P_r & v_{ci}\leq v\leq v_r \\ P_r & v_r\leq v\leq v_{co} \end{cases} \tag{23}$$

where P_r is the rated wind power considered as 15 kW in the system with rated velocity v_r of 7 m/s. The cut-in speed v_{ci} and cut-out speed v_{co} of the wind turbine are taken as 3 m/s and 10 m/s, respectively. The wind speed vs obtained power characteristics curve is shown in Fig. 3.

3.3. Distributed generation bids calculation

The cost function estimation of DG units is calculated as represented in [26] and the cost values are taken from [25]. By considering the depreciation cost (DC) and production cost (PC) of PV, WT, and energy storage devices, the DG bids are given as follows.

$$\begin{cases} B_{DG} = \frac{DC}{PC}P_{DG} \\ DC = \frac{r(1+r)^n}{(1+r)^n-1}IC \end{cases} \tag{24}$$

Here, the interest rate is considered as r and IC is the installation cost

Table 1
Power limits and bid prices of DG units [25].

DG Type	P_{DG}^{min} (kW)	P_{DG}^{max} (kW)	Bid (€/kWh)	SUC/SDC (€)
MT	6	30	0.457	0.96
FC	3	30	0.294	1.65
PV	0	25	2.584	–
WT	0	15	1.073	–
Battery	−30	30	0.38	–
Utility	−30	30	–	–

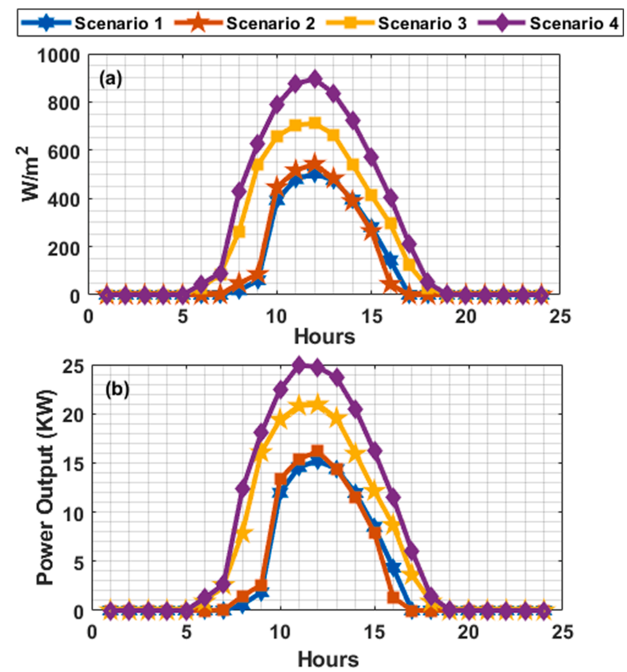

Fig. 4. (a) Solar Irradiance (b) Solar Power Output.

of DG units. Similarly, the bids for MT and FC are calculated as follows.

$$\begin{cases} B_{DG} = C_{fuel}\frac{P_{DG}}{\eta_{DG}} + C_{inv} \\ C_{inv} = DC\frac{P_{DGnom}}{PC} \end{cases} \tag{25}$$

C_{fuel} is the cost of the fuel (€/kWh) required to supply the MT and FC, η_{DG} is the efficiency of MT and FC, and C_{inv} is the annual investment cost for depreciation cost DC, production cost PC, and nominal DG power P_{DGnom}. The DG bid price information and power limitations are given in Table 1.

3.4. Scenario creation for uncertainty models

Stochastic programming is widely applied to address the uncertainty problem of variables like solar PV and WT power output. The scenario-based method is applied in this paper to model the stochastic behavior of variables related to solar PV irradiance and wind speed. The uncertainties in solar PV and WT power output are modeled as [32]:

$$P_{pv,t,s} = P_{pv,t}^{f} + \Delta P_{pv,t,s}; \quad t = 1,\cdots,N_T; \quad s = 1,\cdots,N_s \tag{26}$$

$$P_{wt,t,s} = P_{wt,t}^{f} + \Delta P_{wt,t,s}; \quad t = 1,\cdots,N_T; \quad s = 1,\cdots,N_s \tag{27}$$

where $P_{pv,t}^{f}$, $P_{wt,t}^{f}$, $\Delta P_{pv,t,s}$, and $\Delta P_{wt,t,s}$ are forecasted output power of PV, WT, with their forecast errors respectively. N_T and N_s are time interval quantities and scenario quantities are chosen for the uncertainty model. Most of the previous studies [25,26], have considered the PV and WT

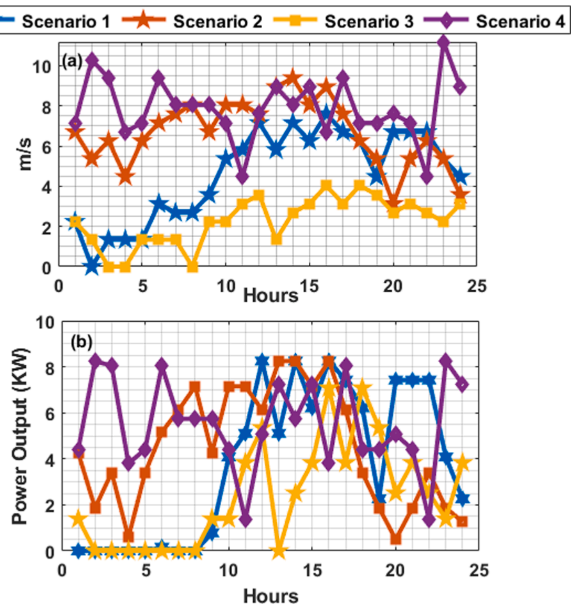

Fig. 5. (a) Wind Speed (b) Wind Power Output.

power output prediction based on a single season and evaluated the results without extending the data to other seasons. However, the authors in this article have considered four distinct seasonal profiles and predicted PV, WT generation based on practical solar irradiation and wind speed. The scenario creation for solar irradiance, wind speed, and power output for PV and WT are shown in Figs. 4 and 5.

4. Methodology

This section deals with the formulation of the generalized framework to solve the MG EMS problem subjected to utility indued DSM with various levels of participation. The details of the QPSO algorithm and its pseudo code to optimize the EMS problem are also presented.

4.1. Three stage stochastic framework for solving MG EMS

Fig. 6 illustrates the proposed three-stage framework to solve the day-ahead scheduling and EMS of grid-connected MG with three distinct features. The uncertainty models of PV and WT are addressed by using a stochastic based scenario generation and reduction technique. The first stage of this framework is the scenario generation module, where a random variable with a range of (0, 1) is assigned to evaluate PV and WT power output based on the probability distribution function by considering the forecast error. The best possible scenarios generated in this module are given as input to the second feature of the framework along with MG system operational parameters, constraints, load forecast, and DG bid prices.

The second and third stages further implement two strategies: with and without considering DSM participation levels. The LC unit in the MG network will provide the modified load profiles based on the inputs obtained from DSM participation levels. The first strategy solves the EMS problem with the help of the QPSO optimizer without considering the DSM program. The impact of DSM on MG operating costs are studied in the second strategy with various participation levels. Finally, the output of LC by adjusting the non-critical loads is fed to an optimization algorithm with a focus on calculating generation set points and estimation of power exchange between utility, energy storage, and MG. The proposed EMS framework will assist the MG operator for critical decision making and obtain robust solution under PV and WT uncertainties. Further, the customers participating in the DSM program will also get economic benefits.

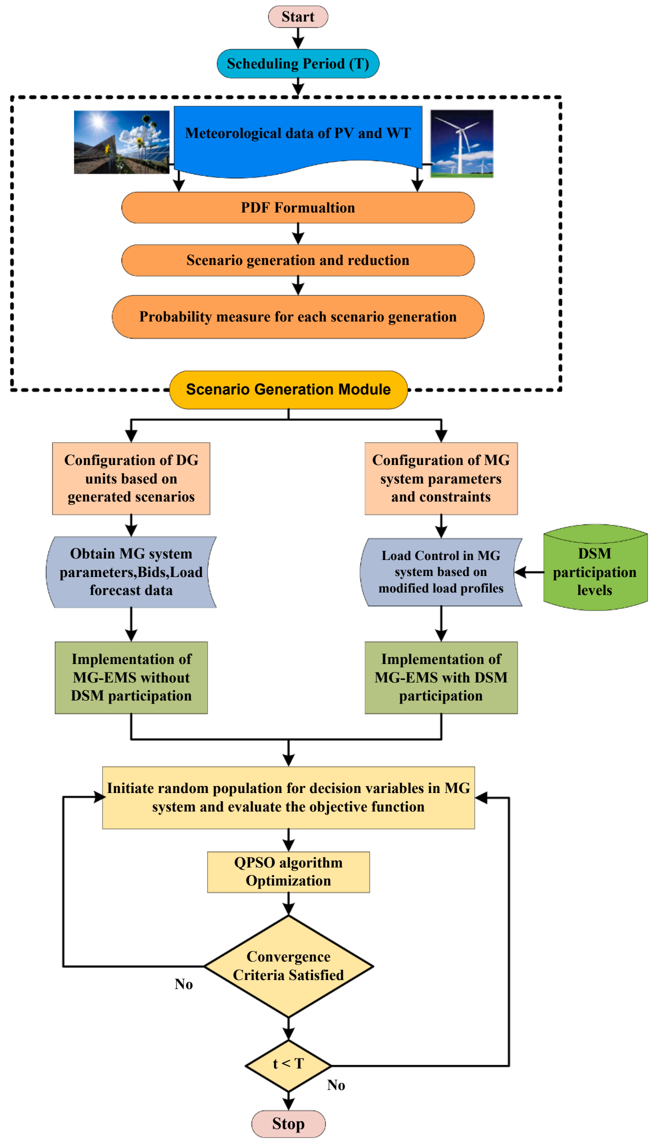

Fig. 6. Proposed framework for MG EMS.

4.2. Quantum particle swarm optimization

Particle swarm optimization (PSO) is one of the popular swarm intelligence based-algorithms which is successfully applied to solve fundamental and critical power system problems like economic dispatch and optimal power flow [27]. Inspired by the theory of quantum mechanics and dynamical analysis of particles, quantum particle swarm optimization (QPSO) was introduced by Sun et al., in [28]. The canonical PSO has a certain limitation when the minor number of particles that fail to converge toward global best, gets discarded by the swarm in the process of particle distribution for succeeding iteration. This will certainly affect the algorithm's global search ability and hence, the concept of mean best is introduced in QPSO to include the lagged particles back in the swarm. Moreover, the QPSO does not require to model the velocity vector of particles and has very few parameters to adjust compared to canonical PSO. The microgrid cost model considered in this paper is formulated as a non-linear optimization problem with multiple constraints. The QPSO algorithm is well suited to solve such non-linear problems including non-smooth and non-convex optimization models effectively. Compared to the canonical PSO, the quantum version has specific features like better stability, accuracy, reliability, with less computational time.

Pseudo code for QPSO
Begin
// Initialize the random population as per the MG system configuration and evaluate current position $x_{i,j}$, pbest $p_{i,j}$ and gbest G_j. Set t=0 //
while (iter count < max iter)
do
Set $t = t + 1$;
Compute mean best position $mbest_{i,j}(t)$;
Select an appropriate ξ value;
for (i = 1 to M)
for j = 1 to N
φ = rand1(.);
$p_{i,j}(t) = (\varphi.p_{i,j}(t) + (1-\varphi)G_j(t))$;
u = rand2(.);
if (rand3($\cdot$) < 0.5)
$x_{i,j}(t+1) = p_{i,j}(t) + \xi.\lvert mbest_{i,j}(t) - x_{i,j}(t)\rvert.\ln\frac{1}{u}$;
else
$x_{i,j}(t+1) = p_{i,j}(t) - \xi.\lvert mbest_{i,j}(t) - x_{i,j}(t)\rvert.\ln\frac{1}{u}$;
end if
end for
Evaluate the objection function of $x_{i,j}(t+1)$, i.e., the total cost $\mathrm{F}(\chi)$ as per (6).
Update $p_{i,j}(t)$ and G_j
end for
end do
end

Fig. 7. Pseudo code for QPSO algorithm for solving MG EMS.

The state of a particle in QPSO is represented with a wave function $\psi(x,t)$. The probability of the particle appearing at position x in time t can be determined by the probability density function $|\psi(x,t)|^2$. The particle position in each iteration is updated as per (28) and (29).

$$x_{i,j}(t+1) = p_{i,j}(t) \pm \xi\cdot\left|mbest_{i,j}(t) - x_{i,j}(t)\right|\cdot\ln\frac{1}{u} \tag{28}$$

$$p_{i,j}(t) = \left(\varphi.p_{i,j}(t) + (1-\varphi)G_j(t)\right), \quad (1 \le i \le N, 1 \le j \le M) \tag{29}$$

$$\varphi = \frac{c_1 r_1}{c_1 r_1 + c_2 r_2} \tag{30}$$

Each particle out of N particles having a dimension D converges to its local attractor $p = (p_1, p_2, p_3, \cdots, p_D)$ in M iterations. Here, $p_{i,j}$ and G_j denotes the personal best and global best position of i^{th}particle in j^{th}iteration; c_1, c_2 are the acceleration coefficients; $r_1, r_2,$ and$u$ are the normally distributed random numbers within [0, 1]. The mean of the personal best positions $mbest_{i,j}(t)$ is essential to update the lagged particles into the population for every new iteration. In the context of quantum mechanics, the parameter ξ is referred to as contraction–expansion coefficient which is defined as $\xi = 1-(1.0-0.5)k/M$, where k being the current iteration count.

$$mbest_{i,j}(t) = \frac{1}{N}\sum_{i=0,j=1}^{N,M} p_{i,j}(t) = \left(\frac{1}{N}\sum_{i=0}^{N} p_{i,1}(t), \frac{1}{N}\sum_{i=0}^{N} p_{i,2}(t), \cdots, \frac{1}{N}\sum_{i=0}^{N} p_{i,D}(t)\right) \tag{31}$$

The pseudo-code of the QPSO shown in Fig. 7 explains the iterative process in simple steps. First, the system parameters for MG are initiated according to the framework. The initial population of 50 is generated to evaluate the decision variables within the solution search space. Then, the fitness value of each solution is calculated to define personal best and global best for a maximum of 200 iterations. The contraction–expansion coefficient is carefully tuned to avoid premature convergence. The mean best defined during each iteration helps the algorithm to improve the population diversity. The positive sign is assigned to (28) if the randomly created number is less than 0.5 and vice-versa. The stopping criteria for termination of the algorithm are based on convergence and the maximum number of iterations. Finally, the personal best and global best values updated in the converged solution gives the optimal set values of power references for DG units along with the cost calculated for 24 h.

5. Simulation results and discussion

5.1. Simulation evaluation criteria

This section deals with the implementation of the proposed three-stage stochastic framework to analyze the effect of the DSM program on the aforementioned problem on a typical microgrid shown in Fig. 2. The proposed QPSO algorithm was implemented in MATLAB R2020a software with a system configuration of 2.20 GHz, 8.0 GB RAM for 20 trial runs. The population size and iteration count of QPSO are considered as 50 and 200, respectively. To prove the efficacy of the algorithm, QPSO is compared with the popular state of the art algorithms like Differential Evolution (DE), Real-Coded Genetic Algorithm (RCGA), and the standard counterpart of QPSO, i.e., Particle Swarm Optimization (PSO). The algorithm-specific parameters for DE are taken as a crossover probability of 0.7, scaling factor of 0.5. For RCGA, the distribution index for both crossover and mutation is considered as 4 and their respective probabilities are taken as 0.8 and 0.2. The cognitive and social attributes of PSO are taken as 2 and 2, respectively with a maximum inertia weight of 0.89 and the minimum inertia weight of 0.41. Similar to QPSO, the population size and iteration count of DE, RCGA and PSO is considered as 50 and 200, respectively. Five case studies were developed to evaluate the proposed framework and a brief discussion of each case study is presented below.

Case study 1, which is also considered as the base case in this paper deals with the EMS problem with an objective of minimizing total operating costs by employing a QPSO optimizer. In this base case, the impact of power exchange between utility and DG units without implementing the DSM program is examined in terms of operating cost. The residential load in the MG network comprises several controllable loads for flexible load shaping and they can be easily managed when compared to other types of loads. With this regard, the DSM program was implemented to residential loads only [31]. In the interest of observing the impact of the DSM program on MG operating costs, the objective function $\mathrm{F}(\chi)$ is incorporated with a participation level of 5% DSM in case study 2. The remaining case studies 3, 4, and 5 are an

Table 2
Microgrid operating costs in €ct for the base case.

Algorithm	Scenario 1	Scenario 2	Scenario 3	Scenario 4	Computational Time (s)
DE	281.89	334.03	379.84	416.21	41.84
RCGA	255.54	298.51	374.62	412.18	38.29
PSO	229.79	267.10	350.13	392.14	37.45
QPSO	229.81	267.65	350.16	392.16	22.29

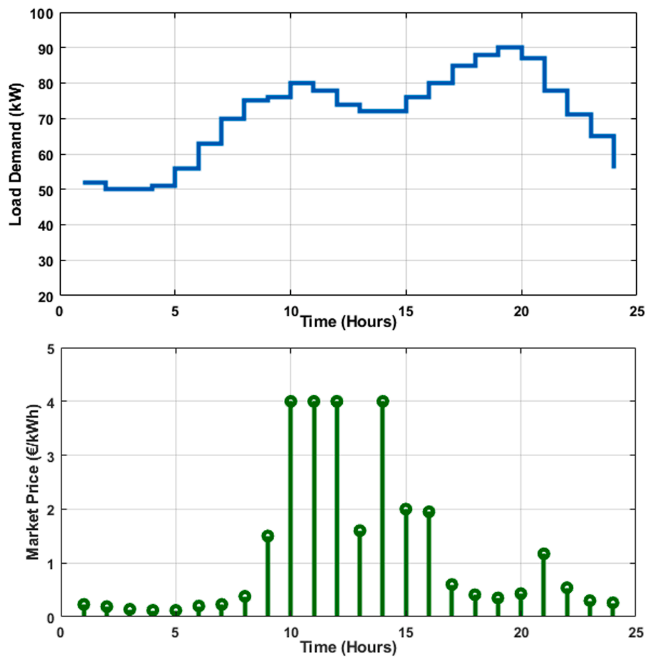

Fig. 8. Utility market price and Load demand.

extension of case 2 with 10%, 15%, and 20% DSM participation levels, respectively. The corresponding simulation results with all four scenarios including the computational time are tabulated in Table 2 for the base case.

The model considered in this paper contains four scenarios for solar PV and WT power generation. As already discussed in Section 3.3, the calculation of bid costs for all DG units with maximum and minimum power constraints is decided prior to the implementation of the proposed framework. Fig. 8 depicts the utility market price and forecasted load data [25] for day-ahead scheduling. The final decision over the power trading between the MG and utility is taken by MGCC at each hour. The objective function for the EMS problem is incorporated with the DSM program with different participation levels of forecasted load. The effect of DSM on reducing the total operating cost of MG under created real-time scenarios is evaluated for all participation levels in a 24-hour time interval.

Four assumptions have been considered for the simulation studies: (1) All the loads in the network are electrical and no heating load is considered. (2) Maximum power is extracted from renewable sources during each time interval to exploit the benefits to the MG operator in all scenarios. (3) The power output at the point of common coupling in the MG network is at unity power factor. (4) The dynamics of the loads in grid-connected microgrid are not considered. However, the flexible load shaping strategy of controllable loads is investigated. Based on these assumptions, five case studies are designed to evaluate the proposed framework. The optimal generation set points along with the hourly operating cost of the MG network evaluated for the designed case studies are presented below.

5.2. Simulation results for test cases

5.2.1. Case 1: Base case without DSM implementation

Fig. 9 represents the optimal dispatch of DG sources evaluated for chosen scenarios without considering the DSM. As the penetration of PV and WT increases in each scenario, the MG utilizes the renewable sources to the maximum possible extent. During the off-peak demand from 1 to 8 h, the battery gets charged as the utility market price is low.

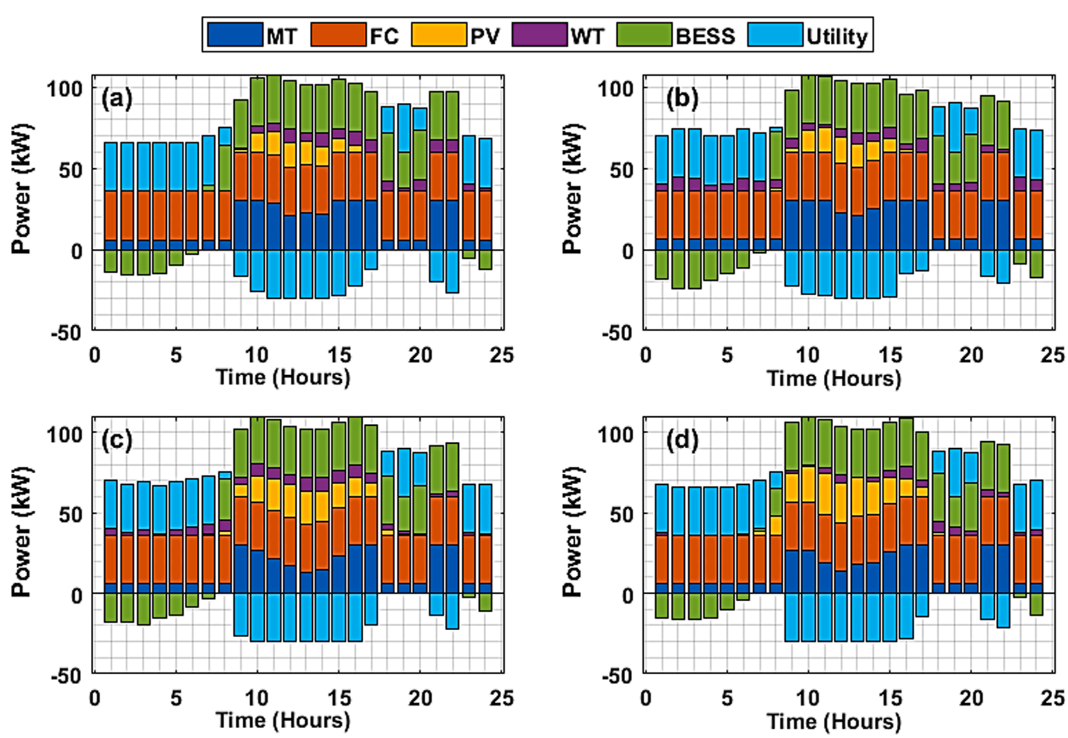

Fig. 9. Simulation results of Case 1 with (a) Scenario 1 (b) Scenario 2 (c) Scenario 3 (d) Scenario 4.

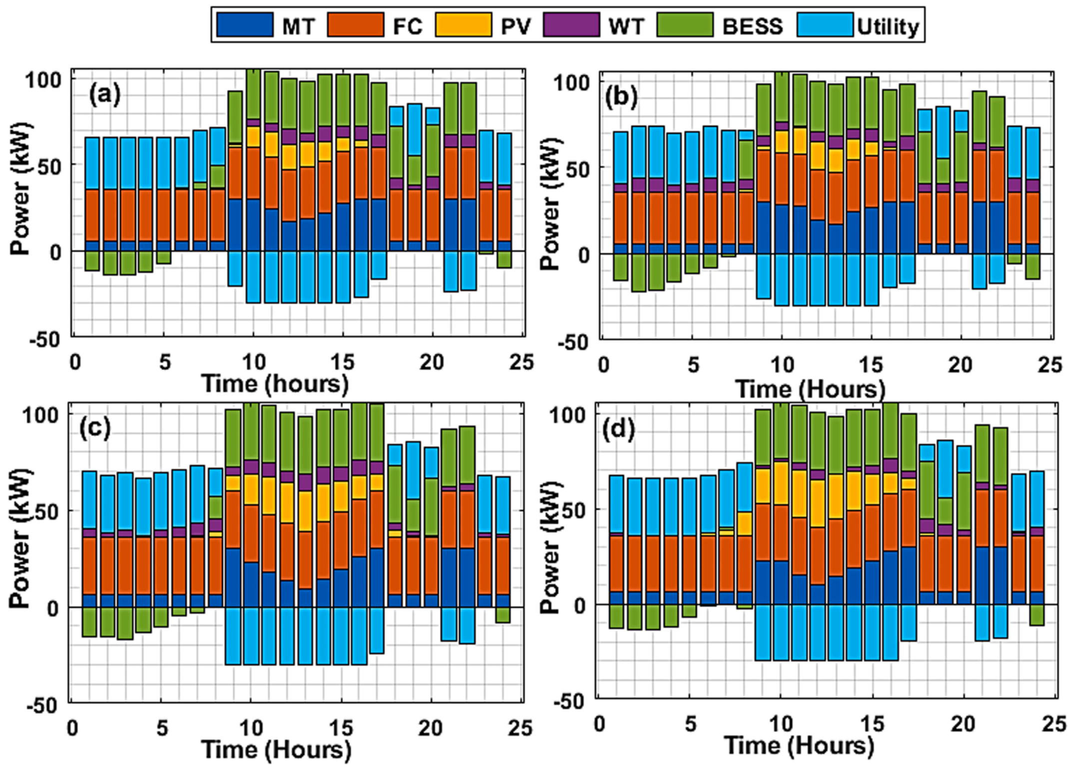

Fig. 10. Simulation results of Case 2 with (a) Scenario 1 (b) Scenario 2 (c) Scenario 3 (d) Scenario 4.

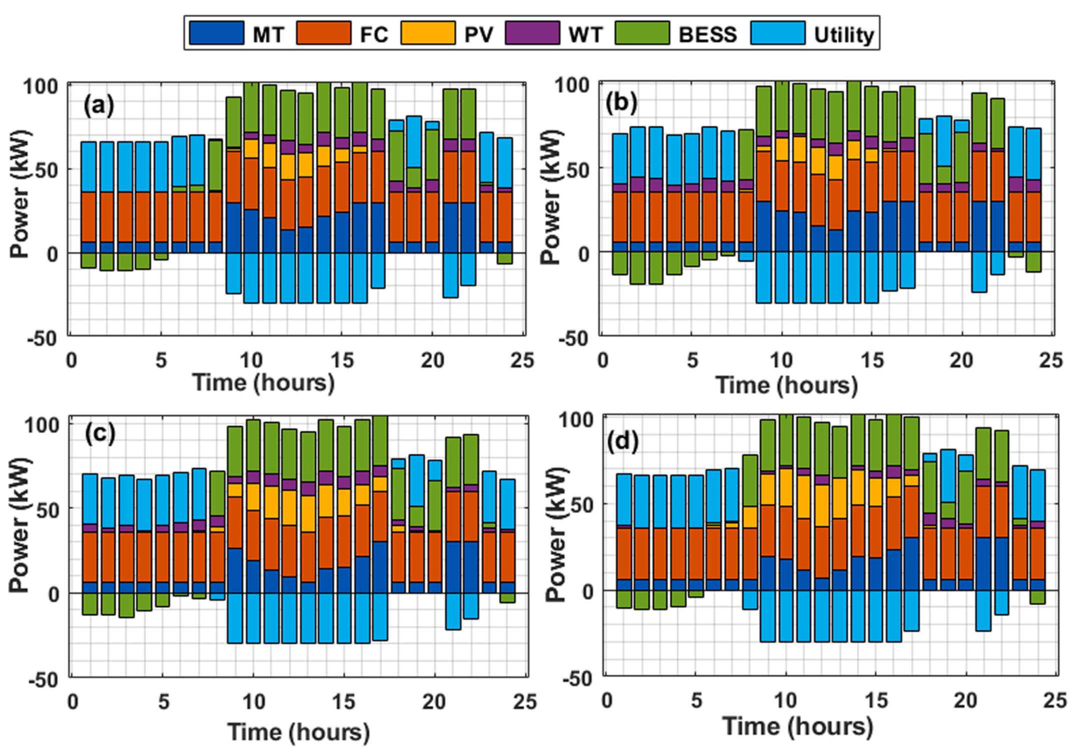

Fig. 11. Simulation results of Case 3 with (a) Scenario 1 (b) Scenario 2 (c) Scenario 3 (d) Scenario 4.

In Fig. 9(a), it is observed that the WT contributes to MG during peak demand from 21 to 22 h, increasing the energy export to the utility in the first scenario. This results in an overall reduction in operating costs for scenario 1 compared to other scenarios. In all scenarios, the power export to utility is restricted to a minimum value during the peak demand between 17 and 22 h, to exploit maximum benefit from the battery. The operating cost of generating units in MG is obtained as 229.81, 267.65, 350.16, 392.16 €ct/kWh for four scenarios, respectively. It is evident that the contribution of renewable power output gradually increases from each scenario resulting in an increment of total

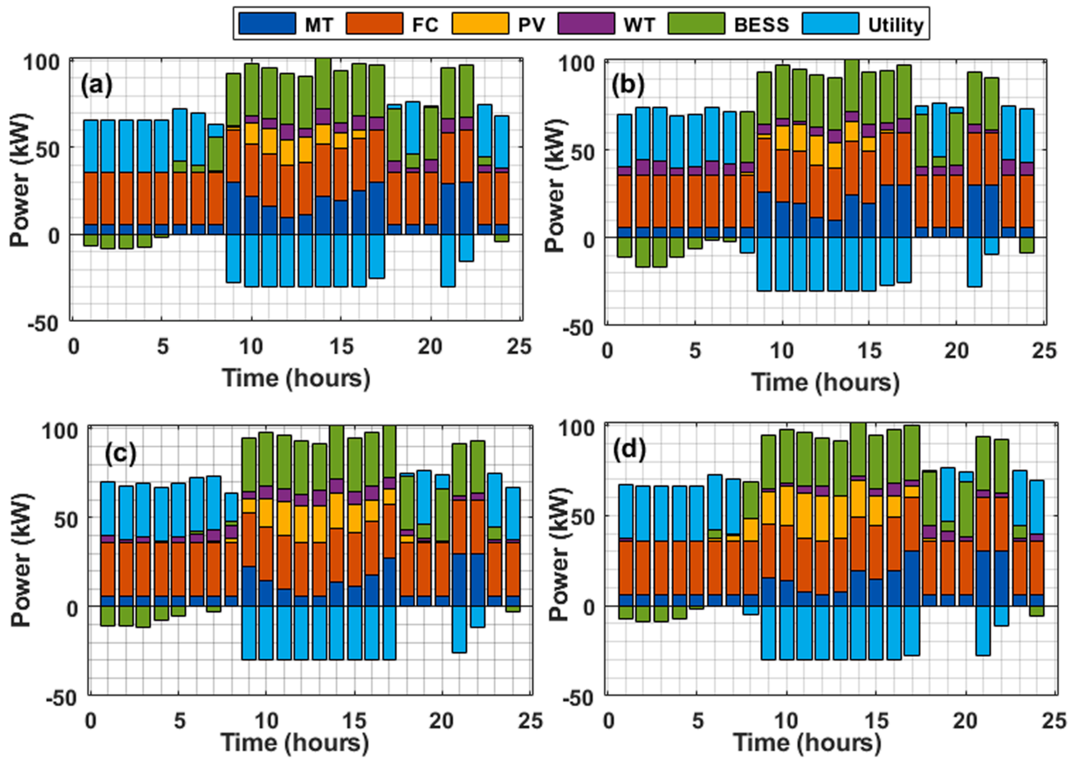

Fig. 12. Simulation results of Case 4 with (a) Scenario 1 (b) Scenario 2 (c) Scenario 3 (d) Scenario 4.

operating cost due to high bid prices of PV and WT among other DG units.

5.2.2. Case 2: Implementation of DSM with 5% load participation

The effect of the implementation of DSM on MG EMS with a participation level of 5% is studied in Case 2. Fig. 10 represents the best power dispatch solution using the QPSO algorithm for all scenarios and it is evident that the overall operating cost got reduced when compared to Case 1. When the utility market price is low, the battery is scheduled for charging during 0–6 and 23–24 h, respectively. The stored energy of the battery is consumed during peak hours to supply the load and exporting the rest of the energy to the utility. Further, it is also observed

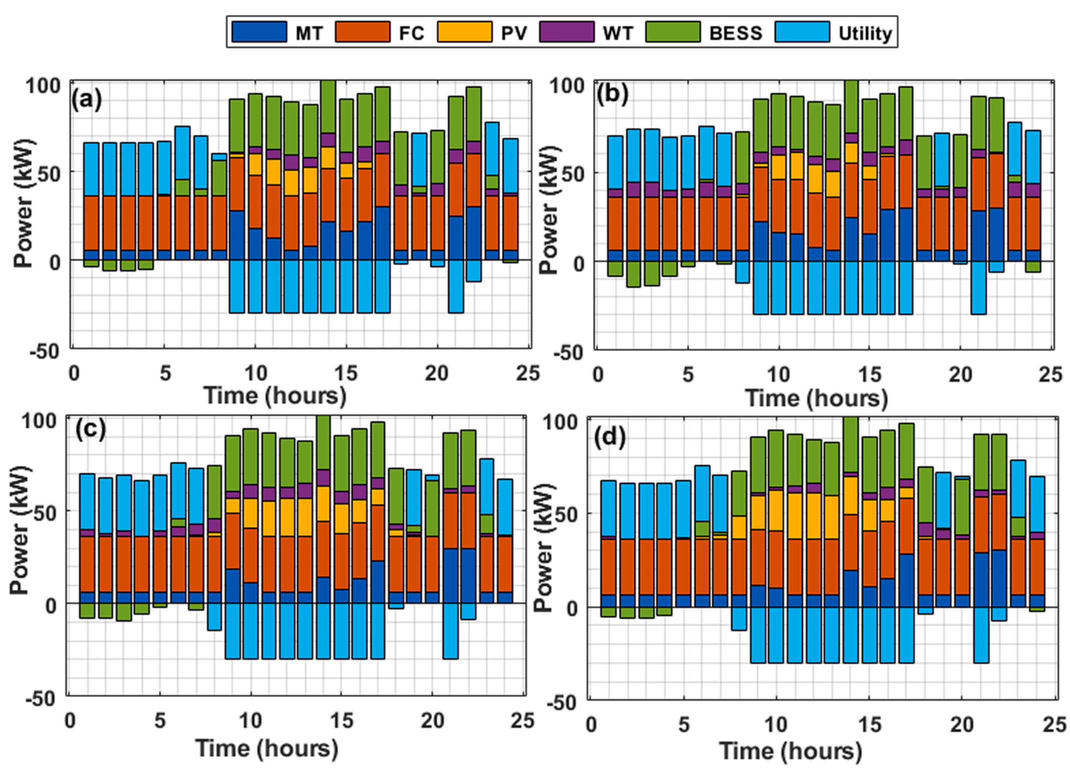

Fig. 13. Simulation results of Case 5 with (a) Scenario 1 (b) Scenario 2 (c) Scenario 3 (d) Scenario 4.

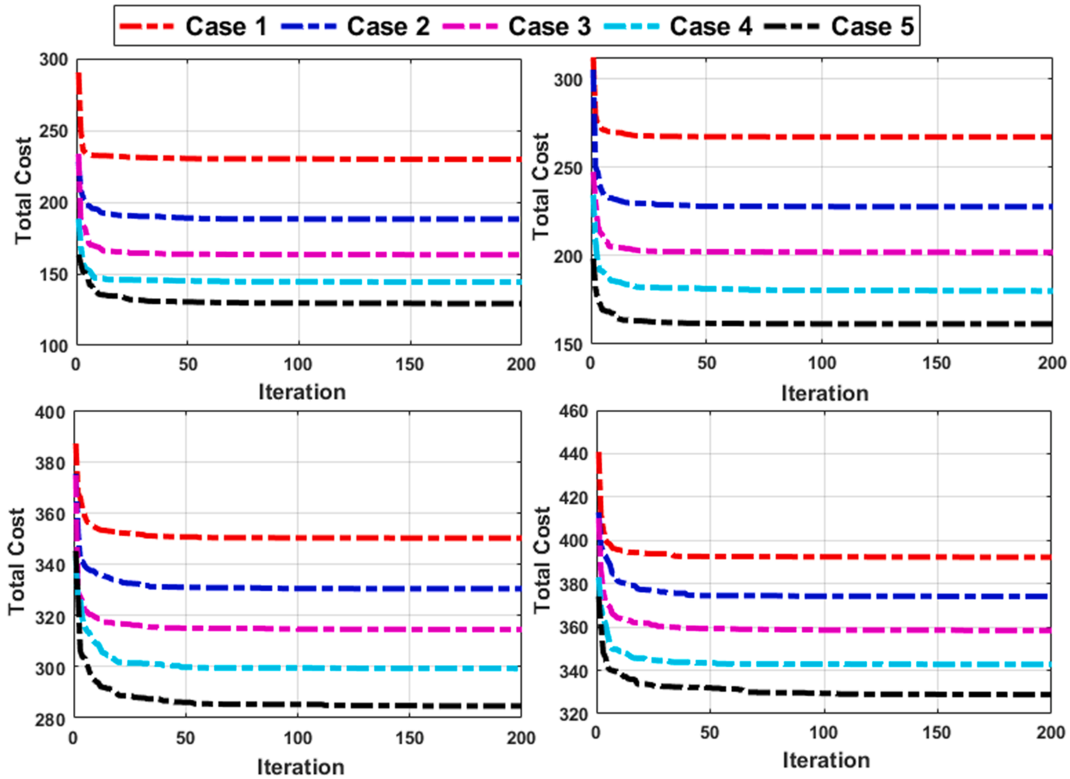

Fig. 14. Convergence characteristics of QPSO algorithm for (a) Scenario 1 (b) Scenario 2 (c) Scenario 3 (d) Scenario 4.

that the maximum energy is exported to the utility as the renewable penetration is more in scenario 4 as shown in Fig. 10(d) compare to Fig. 10(d). The operating costs evaluated for this case are 188.07, 227.65, 330.35, and 374.17 €ct for all four scenarios, respectively. The percentage reduction in terms of cost for Case 1 and Case 2 is 18.16%, 14.13%, 5.65%, and 4.58%.

5.2.3. Case 3: Implementation of DSM with 10% load participation

The stochastic EMS incorporated with DSM of 10% participation level from residential loads is shown in Fig. 11. From the obtained results, one can notice that the FC is utilized to the maximum limit of 30 kW due to it's lowest bid price among other DG units. On other hand, the MT power consumption is restricted to its minimum limit of 3 kW during the first 8 h, 18–20 and 23–24 h, respectively since it has a higher bid compared to utility market price. The overall usage of MT is further optimized in Case 3 when compared to Case 1 in hours 11–13 when the generation from renewables is higher especially in scenario 4. The operating costs evaluated in Case 3 are 163.20, 201.92, 314.46, and 358.31 €ct for all scenarios, respectively. With the implementation of 10% DSM, the percentage reduction in terms of cost is 28.98%, 24.55%, 10.19%, and 8.63% when compared to Case 1.

5.2.4. Case 4: Implementation of DSM with 15% load participation

Fig. 12 shows the optimal solution of the power dispatch with consideration of 15% DSM participation level. The results obtained in Case 4 shows that the scheduled power from all DG units are optimized to an extent that the MG will reduce importing power from the utility during peak demand hours and overall export energy is further increased when compared to previous cases. The objective function values evaluated in Case 4 are 144.23, 180.03, 299.27, and 342.77 €ct for all scenarios, respectively. The operating costs are further reduced to 37.23%, 32.73%, 14.53%, and 12.59% compared to the case when DSM participation is not considered.

Table 3
Microgrid operating costs in €ct with different DSM participation levels.

	Scenario 1	Scenario 2	Scenario 3	Scenario 4
Case 1	229.81	267.65	350.16	392.16
Case 2	188.07	227.65	330.35	374.17
Case 3	163.20	201.92	314.46	358.31
Case 4	144.23	180.03	299.27	342.77
Case 5	129.12	161.38	284.64	328.86

5.2.5. Case 5: Implementation of DSM with 20% load participation

It can be concluded that the overall MG operational cost is obtained lowest in Case 5 with a DSM participation level of 20% compared to all previous cases. With higher residential load participation levels of DSM, the operating cost value is further optimized against without DSM. From Fig. 13, it is observed that the MG operator can export more power to the utility during peak hours by extracting maximum energy from renewables in Case 5 when compared to all previous cases. The best results obtained in Case 5 are 129.12, 161.38, 284.64, 328.86 €ct for all scenarios, respectively. The percentage reduction of operating costs with 20% DSM participation is 43.81%, 39.70%, 18.71%, 16.14%. Finally, when compared to all simulation results that are evaluated in this work, the optimized result is obtained for scenario 1 of Case 5 with the lowest operating cost of 129.12 €ct.

The performance of QPSO optimizer in terms of convergence characteristics is shown in Fig. 14. According to the obtained result, there is a considerable amount of reduction in the MG operating cost as the DSM participation level increases. The objective function converges to the optimal value in very few iterations in all scenarios. The comparison of simulation results without and with DSM participation levels is shown in Table 3.

DSM program implementation provides the flexible load pattern to match with the generation profile, through shifting controllable loads towards the intervals with off-peak hours. As per the obtained results, the daily cost savings for the MG operator are 41.74, 66.61, 85.58, and

Table 4
. Daily cost savings of MG operator with different DSM participation levels.

	Scenario 1	Scenario 2	Scenario 3	Scenario 4
5% DSM	41.74	40	19.81	17.99
10% DSM	66.61	65.73	35.7	33.85
15% DSM	85.58	87.62	50.89	49.39
20% DSM	100.69	106.27	65.52	63.3

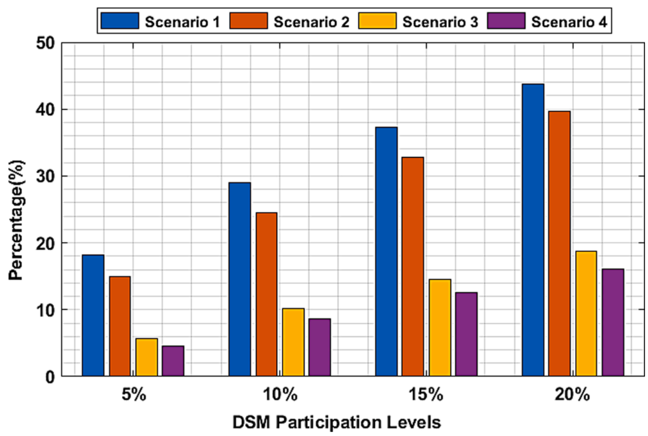

Fig. 15. Cost savings with different DSM participation levels.

100.69 €ct, respectively for different DSM participation levels in the first scenario as shown in Table 4. The daily cost savings in terms of percentage for all scenarios is shown in Fig. 15. A brief comparative analysis of hourly optimal scheduling of MG system with and without the implementation of DSM program is conducted and is given in Table 5. From this analysis, we can conclude that the MG operator can reduce the daily operating cost and also, could be able to achieve higher financial savings throughout the year.

6. Conclusion

In this paper, a new microgrid operation and energy management problem subjected to utility induced demand-side management program is solved. The novel three-stage scenario-based framework is proposed to address the uncertainties involved with renewable sources while solving the optimal scheduling problem with demand-side management over a 24-hour horizon. A stochastic model for solar photovoltaic and wind turbine systems operating in a grid-connected microgrid with four scenarios is created. To investigate the impact of demand-side management on the microgrid, four residential load participation levels of 5%, 10%, 15%, and 20% were evaluated, and results are analyzed with all scenarios. The obtained simulation results prove the efficacy of the Quantum Particle Swarm optimization approach to yield techno-economic benefits for both utility and microgrid operators. Among all the case studies considered in this work, the best optimization result is obtained with a higher demand-side management participation level of 20%. The overall cost reduction of 43.81%, 39.70%, 18.71%, and 16.14% is achieved for all four scenarios, respectively when compared

Table 5
. Comparison of optimal solution with and without DSM participation.

	Case 1							Case 5						
Time	MT	FC	PV	WT	BESS	Utility	Cost	MT	FC	PV	WT	BESS	Utility	Cost
1	6.00	30	0.00	0.00	-14.00	30.00	13.14	6.00	30	0.00	0.00	-3.60	30.00	17.09
2	6.00	30	0.00	0.00	-16.00	30.00	11.18	6.00	30	0.00	0.00	-6.00	30.00	14.98
3	6.00	30	0.00	0.00	-16.00	30.00	9.68	6.00	30	0.00	0.00	-6.00	30.00	13.48
4	6.00	30	0.00	0.00	-15.00	30.00	9.46	6.00	30	0.00	0.00	-4.80	30.00	13.34
5	6.00	30	0.00	0.00	-10.00	30.00	11.36	6.00	30	0.00	0.00	1.20	30.00	15.62
6	6.00	30	0.00	0.16	-3.16	30.00	16.53	6.00	30	0.00	0.16	9.44	30.00	21.32
7	6.00	30	0.00	0.00	4.00	30.00	19.98	6.00	30	0.00	0.00	4.00	30.00	19.98
8	6.00	30	0.57	0.00	28.02	10.40	27.65	6.00	30	0.57	0.00	19.66	3.76	21.95
9	30.00	30	1.85	0.78	30.00	-16.63	14.60	28.17	30	1.85	0.78	30.00	-30.00	-6.30
10	30.00	30	11.97	4.08	30.00	-26.05	-34.96	17.95	30	11.97	4.08	30.00	-30.00	-56.26
11	28.31	30	14.58	5.11	30.00	-30.00	-43.69	12.70	30	14.58	5.11	30.00	-29.99	-50.78
12	20.56	30	15.22	8.25	29.96	-30.00	-42.20	6.00	30	15.22	8.25	29.73	-30.00	-48.96
13	22.52	30	14.37	5.11	30.00	-30.00	25.13	8.12	30	14.37	5.11	30.00	-30.00	18.55
14	21.82	30	11.93	8.25	30.00	-30.00	-50.12	21.81	30	11.93	8.25	30.00	-30.00	-50.12
15	30.00	30	8.50	6.22	30.00	-28.72	5.13	16.09	30	8.50	6.22	30.00	-30.00	-3.80
16	30.00	30	4.35	8.25	30.00	-22.60	9.95	21.40	30	4.35	8.25	30.00	-30.00	-8.42
17	30.00	30	0.00	7.42	30.00	-12.42	34.44	30.00	30	0.00	7.42	30.00	-29.42	24.24
18	6.00	30	0.00	6.22	30.00	15.78	36.11	6.00	30	0.00	6.22	30.00	-1.82	28.89
19	6.00	30	0.00	2.26	21.74	30.00	32.75	6.00	30	0.00	2.26	3.74	30.00	25.91
20	6.00	30	0.00	7.42	30.00	13.58	36.76	6.00	30	0.00	7.42	30.00	-3.82	29.28
21	30.00	30	0.00	7.42	30.00	-19.42	19.17	24.98	30	0.00	7.42	30.00	-30.00	4.50
22	30.00	30	0.00	7.42	30.00	-26.42	27.62	30.00	30	0.00	7.42	30.00	-12.22	35.29
23	6.00	30	0.00	4.08	-5.08	30.00	23.01	6.00	30	0.00	4.08	7.92	30.00	27.95
24	6.00	30	0.00	2.26	-12.26	30.00	17.13	6.00	30	0.00	2.26	-1.06	30.00	21.38
Total Cost							229.81	Total Cost						129.12

to the case without demand-side management participation. The applications of the proposed framework are threefold: The flexible load shaping of non-critical loads in the system improves the load factor and helps the microgrid operator to manage the peak loads effectively. Since energy management is a continuous monitoring process, a significant restriction of peak demand reduces the investment in transmission and distribution corridors. The implementation of demand-side management also helps the energy managers of the utility companies to collect and analyze the load participation profiles to develop new energy policies and to provide operational flexibility to the grid. Finally, the successful implementation of such a strategy boost the publicly owned utilities in the developing nations, which creates real-time energy trading opportunities.

CRediT authorship contribution statement

R. Seshu Kumar: Conceptualization, Methodology, Software, Visualization, Investigation, Writing - original draft. **L. Phani Raghav:** Data curation, Software, Validation. **D. Koteswara Raju:** Project administration, Supervision, Resources, Writing - review & editing. **Arvind R. Singh:** Supervision, Writing - review & editing.

Declaration of Competing Interest

The authors declare that they have no known competing financial interests or personal relationships that could have appeared to influence the work reported in this paper.

References

[1] Katiraei F, Iravani R, Hatziargyriou N, Dimeas A. Microgrids management. IEEE Power Energy Mag 2008;6(3):54–65. https://doi.org/10.1109/MPE.2008.918702.

[2] Meng L, Sanseverino ER, Luna A, Dragicevic T, Vasquez JC, Guerrero JM. Microgrid supervisory controllers and energy management systems: A literature review. Renew Sustain Energy Rev 2016;60:1263–73. https://doi.org/10.1016/j.rser.2016.03.003.

[3] Jiang Q, Xue M, Geng G. Energy management of microgrid in grid-connected and stand-alone modes. IEEE Trans Power Syst 2013;28(3):3380–9. https://doi.org/10.1109/TPWRS.2013.2244104.

[4] Papari B, Edrington CS, Bhattacharya I, Radman G. Effective energy management of hybrid AC–DC microgrids with storage devices. IEEE Trans Smart Grid 2019;10 (1):193–203. https://doi.org/10.1109/TSG.2017.2736789.

[5] Kim HJ, Kim MK, Lee JW. A two-stage stochastic p-robust optimal energy trading management in microgrid operation considering uncertainty with hybrid demand response. Int J Electr Power Energy Syst 2021;124. https://doi.org/10.1016/j.ijepes.2020.106422.

[6] Poolla C, Ishihara AK, Milito R. Designing near-optimal policies for energy management in a stochastic environment. Appl Energy 2019;242:1725–37. https://doi.org/10.1016/j.apenergy.2019.01.228.

[7] Elattar EE, ElSayed SK. Probabilistic energy management with emission of renewable micro-grids including storage devices based on efficient salp swarm algorithm. Renewable Energy 2020;153:23–35. https://doi.org/10.1016/j.renene.2020.01.144.

[8] Luo Liang, Abdulkareem Sarkew S, Rezvani Alireza, Miveh Mohammad Reza, Samad Sarminah, Aljojo Nahla, Pazhoohesh Mehdi. Optimal scheduling of a renewable based microgrid considering photovoltaic system and battery energy storage under uncertainty. J Energy Storage 2020;28. https://doi.org/10.1016/j.est.2020.101306.

[9] Giraldo JS, Castrillon JA, López JC, Rider MJ, Castro CA. Microgrids energy management using robust convex programming. IEEE Trans Smart Grid 2019;10 (4):4520–30. https://doi.org/10.1109/TSG.2018.2863049.

[10] Moretti Luca, Martelli Emanuele, Manzolini Giampaolo. An efficient robust optimization model for the unit commitment and dispatch of multi-energy systems and microgrids. Appl Energy 2020;261. https://doi.org/10.1016/j.apenergy.2019.113859.

[11] Yan J, Menghwar M, Asghar E, Panjwani Manoj Kumar, Liu Yongqian. Real-time energy management for a smart-community microgrid with battery swapping and renewables. Appl Energy 2019;238:180–94. https://doi.org/10.1016/j.apenergy.2018.12.078.

[12] Nikmehr N, Najafi-Ravadanegh S, Khodaei A. Probabilistic optimal scheduling of networked microgrids considering time-based demand response programs under uncertainty. Appl Energy 2017;198:267–79. https://doi.org/10.1016/j.apenergy.2017.04.071.

[13] Wang D, Qiu J, Reedman L, Meng Ke, Lei Lai Loi. Two-stage energy management for networked microgrids with high renewable penetration. Appl Energy 2018;226: 39–48. https://doi.org/10.1016/j.apenergy.2018.05.112.

[14] Hossain Md Alamgir, Pota Hemanshu Roy, Squartini Stefano, Zaman Forhad, Guerrero Josep M. Energy scheduling of community microgrid with battery cost using particle swarm optimization. Appl Energy 2019;254. https://doi.org/10.1016/j.apenergy.2019.113723.

[15] Venayagamoorthy GK, Sharma RK, Gautam PK, Ahmadi A. Dynamic Energy management system for a smart microgrid. IEEE Trans Neural Networks Learn Syst 2016;27(8):1643–56. https://doi.org/10.1109/TNNLS.2016.2514358.

[16] Sujil A, Kumar R, Bansal RC. FCM Clustering-ANFIS-based PV and wind generation forecasting agent for energy management in a smart microgrid. J Eng 2019;7 2019 (18):4852–7. https://doi.org/10.1049/joe.2018.9323.

[17] Murty VVSN, Kumar A. Multi-objective energy management in microgrids with hybrid energy sources and battery energy storage systems. Prot Control Mod Power Syst 2020;5(2). https://doi.org/10.1186/s41601-019-0147-z.

[18] Amrollahi Mohammad Hossein, Bathaee Seyyed Mohammad Taghi. Techno-economic optimization of hybrid photovoltaic/wind generation together with energy storage system in a stand-alone micro-grid subjected to demand response. Appl Energy 2017;202:66–77. https://doi.org/10.1016/j.apenergy.2017.05.116.

[19] Ju C, Wang P, Goel L, Xu Y. A two-layer energy management system for microgrids with hybrid energy storage considering degradation costs. IEEE Trans Smart Grid 2018;9(6):6047–57. https://doi.org/10.1109/TSG.2017.2703126.

[20] Mohammadjafari Mehdi, Ebrahimi Reza, Darabad Vahid Parvin. Optimal energy management of a microgrid incorporating a novel efficient demand response and battery storage system. J Electr Eng Technol 2020;15(2). https://doi.org/10.1007/s42835-020-00345-5.

[21] Shaghaghi-shahr Gholamreza, Sedighizadeh Mostafa, Mohammadreza Aghamohammadi, Esmaili Masoud. Optimal generation scheduling in microgrids using mixed-integer second-order cone programming. Eng Optimiz 2020:020. https://doi.org/10.1080/0305215X.2019.1695790.

[22] Alahmed Ahmed S, Al-Muhaini Mohammad M. An intelligent load priority list–based integrated energy management system in microgrids. Electr Power Syst Res 2020;185. https://doi.org/10.1016/j.epsr.2020.106404.

[23] Zheng Y, Jenkins BM, Kornbluth K, Kendall A, Træholt C. Optimization of a biomass-integrated renewable energy microgrid with demand side management under uncertainty. Appl Energy 2018;230:836–44. https://doi.org/10.1016/j.apenergy.2018.09.015.

[24] Mehdizadeh A, Taghizadegan N, Salehi J. Risk-based energy management of renewable-based microgrid using information gap decision theory in the presence of peak load management. Appl Energy 2018;211:617–30. https://doi.org/10.1016/j.apenergy.2017.11.084.

[25] Amjad Anvari Moghaddam, Seifi Alireza, Niknam Taher, Pahlavani Mohammad Reza Alizadeh. Multi-objective operation management of a renewable MG (micro-grid) with back-up micro-turbine/fuel cell/battery hybrid power source. Energy 2011;36(11):6490–507. https://doi.org/10.1016/j.energy.2011.09.017.

[26] Radosavljević J, Jevtić M, Klimenta D. Energy and operation management of a microgrid using particle swarm optimization. Eng Optim 2015;48(5):811–30. https://doi.org/10.1080/0305215X.2015.1057135.

[27] Lolla PR, Rangu SK, Dhenuvakonda KR, Singh AR. A comprehensive review of soft computing algorithms for optimal generation scheduling. Int J Energy Res 2020: 1–20. https://doi.org/10.1002/er.5759.

[28] Sun J, Feng B, Xu W. Particle swarm optimization with particles having quantum behavior. In: Proceedings of the 2004 IEEE congress on evolutionary computation, Piscataway, NJ; 2004. p. 325–31.

[29] Logenthiran T, Srinivasan D, Shun TZ. Demand side management in smart grid using heuristic optimization. IEEE Trans Smart Grid 2012;3(3):1244–52. https://doi.org/10.1109/TSG.2012.2195686.

[30] Rangu SK, Lolla PR, Dhenuvakonda KR, Singh AR. Recent trends in power management strategies for optimal operation of distributed energy resources in microgrids: A comprehensive review. Int J Energy Res 2020:1–23. https://doi.org/10.1002/er.5649.

[31] Lokeshgupta B, Sivasubramani S. Multi-objective dynamic economic and emission dispatch with demand side management. Int J Electr Power Energy Syst 2018;97: 334–43. https://doi.org/10.1016/j.ijepes.2017.11.020.

[32] Wu L, Shahidehpour M, Li T. Stochastic security-constrained unit commitment. IEEE Trans Power Syst 2007;22(2):800–11. https://doi.org/10.1109/TPWRS.2007.894843.

[33] Korkas CD, Baldi S, Michailidis I, Kosmatopoulos EB. Intelligent energy and thermal comfort management in grid-connected microgrids with heterogeneous occupancy schedule. Appl Energy 2015;149:194–203. https://doi.org/10.1016/j.apenergy.2015.01.145.

[34] Zhu Junjie, Huang Shengjun, Liu Yajie, Lei Hongtao, Sang Bo. Optimal energy management for grid-connected microgrids via expected-scenario-oriented robust optimization. Energy 2021;216. https://doi.org/10.1016/j.energy.2020.119224.

[35] Korkas CD, Baldi S, Kosmatopoulos EB. Grid-connected microgrids: demand management via distributed control and human-in-the-loop optimization. Adv Renew Energies Power Technol 2018:315–44. https://doi.org/10.1016/B978-0-12-813185-5.00025-5.